

LA-UR-20-23333

Approved for public release; distribution is unlimited.

Title: The Deflagration-to-Detonation Transition in Two Dimensions

Author(s): Heatwole, Eric Mann  
Feagin, Trevor Alexander  
Parker, Gary Robert Jr.

Intended for: Report

Issued: 2020-05-01

---

**Disclaimer:**

Los Alamos National Laboratory, an affirmative action/equal opportunity employer, is operated by Triad National Security, LLC for the National Nuclear Security Administration of U.S. Department of Energy under contract 89233218CNA000001. By approving this article, the publisher recognizes that the U.S. Government retains nonexclusive, royalty-free license to publish or reproduce the published form of this contribution, or to allow others to do so, for U.S. Government purposes. Los Alamos National Laboratory requests that the publisher identify this article as work performed under the auspices of the U.S. Department of Energy. Los Alamos National Laboratory strongly supports academic freedom and a researcher's right to publish; as an institution, however, the Laboratory does not endorse the viewpoint of a publication or guarantee its technical correctness.

# The Deflagration-to-Detonation Transition in Two Dimensions

Eric Heatwole, Trevor Feagin and Gary R. Parker  
M-6, LANL

3-10-2020

## 1 Introduction

The Deflagration-to-Detonation Transition (DDT) in one-dimensional porous explosive, where combustion in an explosive transitions to detonation, can be described by the following model [4] [5]. This simplified model proceeds in five steps, as follows: 1) Ignition of the explosive, surface burning. 2) Convective burning, with the flame front penetrating through the porous network of the explosive. This proceeds until the pressure grows high enough to result in choked flow in the pores restricting the convective burn. 3) The choked flow results in the formation of a high-density compact of explosive. This compact is driven into undisturbed material by the pressure of the burning explosive. See Figure 1. 4) The compression of the undisturbed porous explosive by the compact leads to the ignition of a compressive burn. This builds in pressure until a supported shock forms. 5) The shock builds in pressure until detonation occurs. See Figures 1 and 2 for an overview of the proceeding steps.

It has been assumed in the past that the same mechanism which drives DDT in the one dimensional case will apply to both two and three dimensions. However, this has never been experimentally verified and it is possible that an entirely new mechanism drives DDT in higher dimensions. In order to test this a series of two dimensional DDT tests were performed to help provide empirical evidence of the mechanism in higher dimensions.

## 2 Experimental Setup

A total of three two dimensional tests were performed, all with slightly different experimental parameters. All tests were performed with the bimodal HMX powder with an initial density of 1.2 g/cm<sup>3</sup>. All test fixtures were made of steel plates with a wedge shaped well machined into it. The explosive was placed in a 3 mm deep inset, with a step to allow a relief machined piece to be fitted into

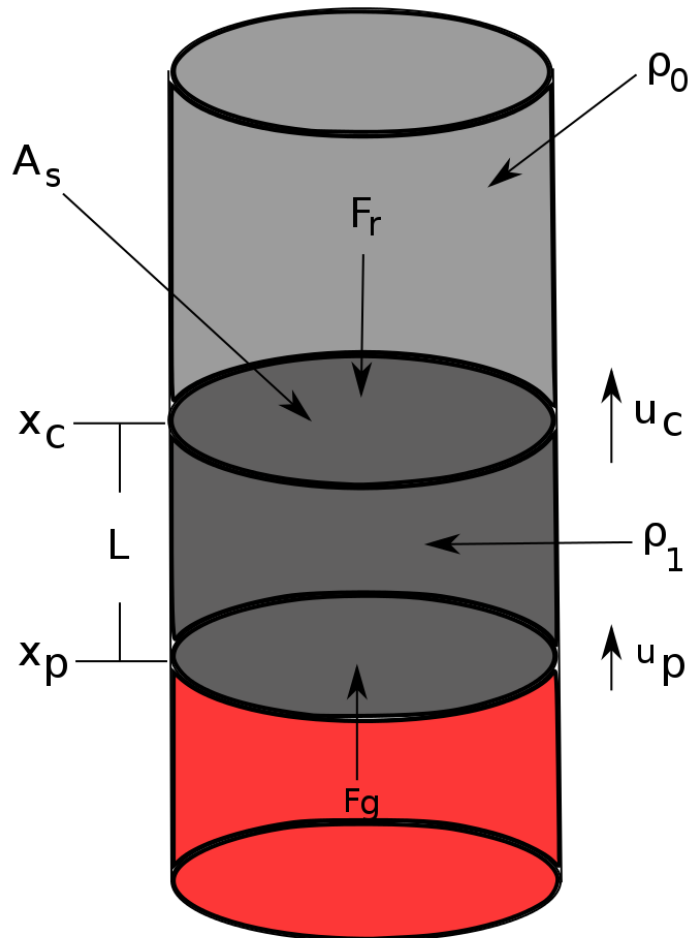


Figure 1: Overview of the simple 1-D DDT model. The burning explosive push the high-density ( $\rho_1$ ) compact of explosive into the lower density ( $\rho_0$ ) undisturbed material with force  $F_g$ . The compact of length,  $L$ , moves at a velocity  $u_p$ , with the leading edge of the compact moving at  $u_c$ .

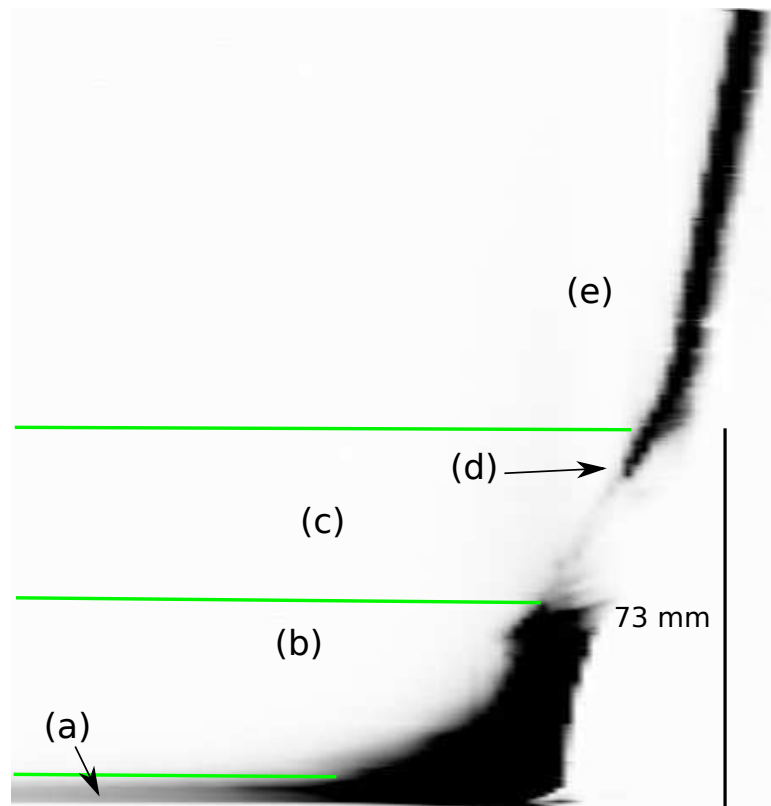


Figure 2: Overview of a streak image illustrating the steps of the DDT process.  
(a) Surface burning of explosive. (b) The convective burn. (c) Formation of the high-density compact. (d) The compressive burn. (e) Detonation.

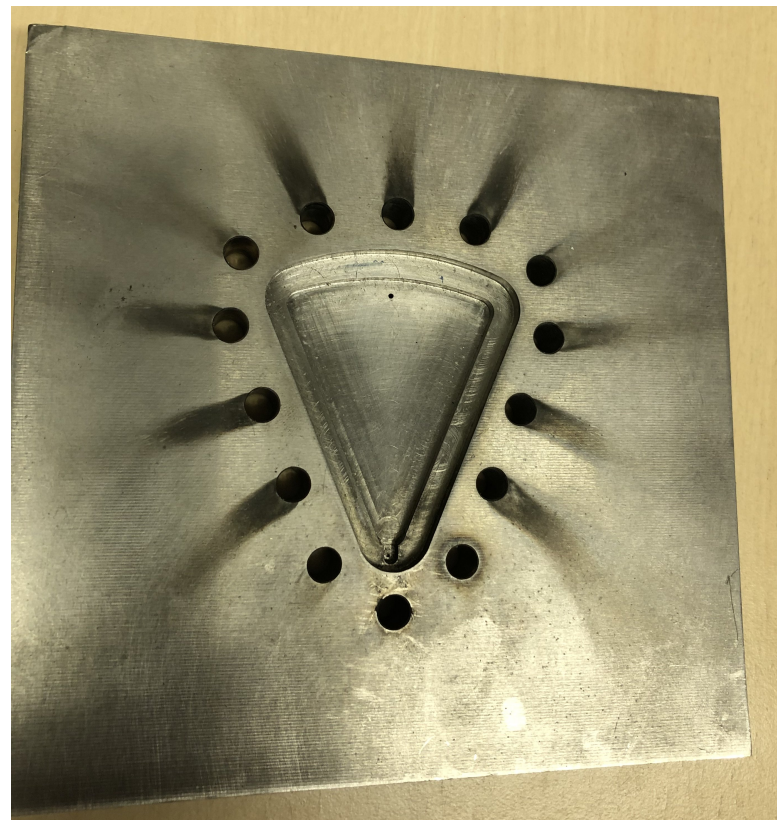


Figure 3: Picture of fixture used in test 2, showing inner well to fill with HMX and step. The fixture is then covered with a polycarbonate plate a steel cover.

the hole to seal the experiment. The narrow end of the wedge had a narrow well machined into it and filled with thermite which was ignited with a 3000 W 1064 nm laser piped in via a 200  $\mu\text{m}$  fiber optic. See Figure 3.

Two of the tests were sealed with a 1 inch thick sheet of polycarbonate to provide optical access, while the third tests was sealed with a steel cover which did not allow optical access but provided greater confinement. The angle and length of the well was also varied. For the tests with optical access, a Phantom 2512 high speed camera was used to observe the DDT mechanism. See Table 1 for an overview.

During the course of this test series a fiber coupled, high-speed, multi-color optical pyrometer was under development [3][2]. In the third test five channels of pyrometry were used, where the fibers were placed 23, 39, 55, 71, and 79 mm from the thermite. While the optical pyrometer failed to obtain temperature

Test	Angle	Length	Optical
1	90	63	Yes
2	60	58	Yes
3	45	82	No

Table 1: Summary of the wedge angle, length and optical access.

data for this test, it was used to measure the time of arrival of the flame front and detonation wave.

### 3 Results and Discussion

While the two tests with optical access failed to transition to detonation, due to the polycarbonate under going plastic failure and lowering the pressure, both exhibited phenomenon associated with the normal one-dimensional DDT mechanism. In particular, the first three steps of the DDT process outlined above can be observed in the optical data. Figures 4 and 5 show montage of images taken from the high-speed video at different steps in the process. In these images, the first row shows the ignition and convective burn as the flame front progresses into the material, steps 1 and 2 of the DDT mechanism. In the second row of images, as the pressure builds, the flame front ceases to convectively burn into the explosive and the remaining material organizes into a arc shaped compact of material, step 3 of the DDT process. At this point, the fixtures begin to leak and there insufficient pressure to proceed to step 4 of the DDT mechanism.

However, as can be seen in the third row, the pressure wave is reflected from the curved rear surface of the wedge and shows visible intensification of the reaction as the pressure wave travels back down the wedge to converge at the ignition. This wave is moving at approximately  $1.3 - 1.6 \text{ mm}/\mu\text{sec}$ , which, if this was a sonic wave in an ideal diatomic gas would correspond to a very conservative  $3400 - 5100 \text{ K}$  temperature gas, which from other work with the DDT would be hotter than expected. This gives some visible evidence that a pressure wave can reflect off a high-impedance surface and cause increase in reaction rate. This could be a possible mechanism for shortening the run length of the DDT mechanism.

The third test did not have optical access and was completely sealed in steel. The optical pyrometer fibers and the steel fixture acting as a witness plate were the only means of diagnosing this test. This test clearly under went the deflagration-to-detonation transition.

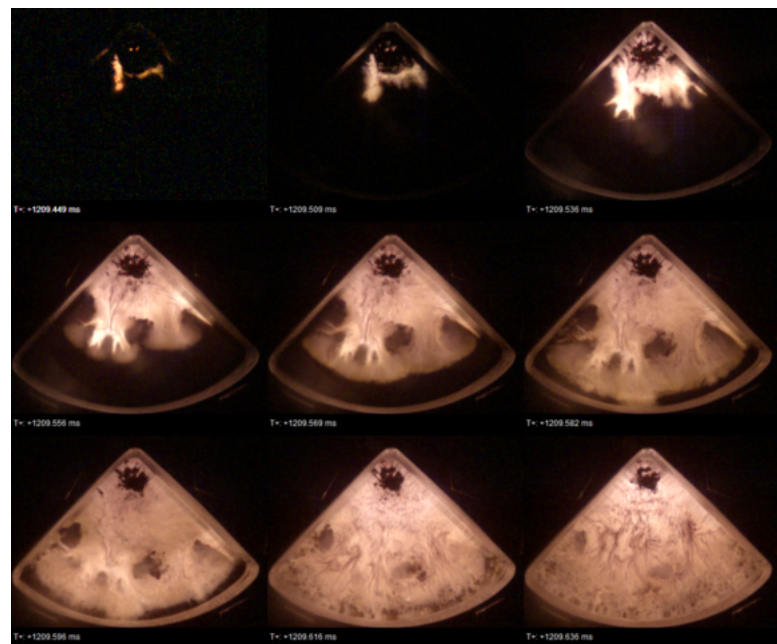


Figure 4: Montage from high-speed video of test 1, showing the first three steps of DDT process. The first row of pictures illustrates the first two steps of DDT, the initial burn and convective burn. The second row illustrates the third step in DDT, the compact formation, while the third row shows the reflection of a pressure wave and its intensification.

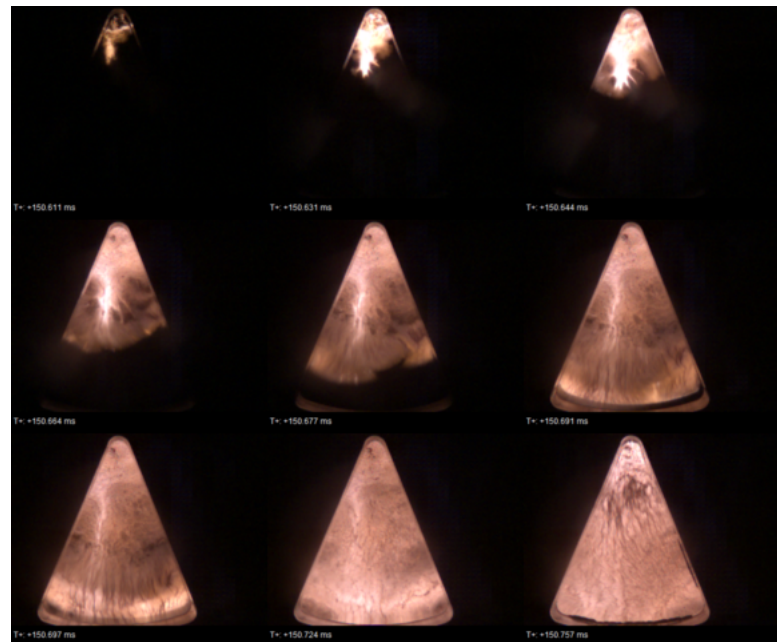


Figure 5: Montage from high-speed video of test 2, showing the first three steps of DDT process. The first row of pictures illustrates the first two steps of DDT, the initial burn and convective burn. The second row illustrates the third step in DDT, the compact formation, while the third row shows the reflection of a pressure wave and its intensification.

Fibers	Delta t ( $\mu$ s)	Velocity (mm/s)	Density (g/cm <sup>3</sup> )
2-3	2.87	5.6	1.02
3-4	2.40	6.6	1.24
4-5	1.18	6.8	1.32

Table 2: Summary of detonation velocity and estimated density from optical pin data. The initial density was 1.2 g/cm<sup>3</sup> with an estimate detonation velocity of 6.3 mm/ $\mu$ s. The first pin velocity is expected to be low since the explosive transition to detonation directly over the second optical pin.

From the witness plate the characteristic blackening which occurs on 1018 steel during the transition to detonation is clearly visible 35 - 42 mm from the ignition. This places the transition directly on top of the second optical fiber. The time of arrival data can then be used to determine the detonation velocity and from that estimate the density of the HMX using the Urizer method [1]. These results are summarized in Table 2.

The optical pin data shows an increasing detonation velocity and estimated density as the detonation moves down the test fixture. This seems to indicate that the material has been compacted some what during the initial phase of the process, which is consistent with the observations from the first two tests, however, this effect is not seen in the one dimensional DDT tests. Also, the run length from ignition to detonation is compatible with the run lengths seen in one dimensional DDT tests with granular HMX [5]. All this seems to indicate that the normal DDT mechanism holds for DDT in this particular two dimensional configuration.

## 4 Conclusion

All three two dimensional DDT tests performed supported the hypothesis that the classical Type I DDT mechanism is valid in a two dimensional configuration. The first two tests with optical access underwent the first three steps of the Type I mechanism, from initial burn, to convective burn, and finally organizing to a compact formation when the confinement fails. The third test had no optical access, which allowed for higher confinement and DDT. This test showed a run length and detonation velocity consistent with one dimensional DDT tests performed with granular HMX.

It also, should be noted that while the first two test failed to DDT they showed a reaction intensification due to a pressure wave reflecting off the back surface of the test fixture. This represents a possible transition mechanism to detonation and the shortening of the run length to detonation.

While these tests seem to indicate that the Type I mechanism holds for this particular setup, well instrumented higher dimension DDT experiments are rarely performed due to the technical difficulties in performing them, especially in a full three dimensional configuration. Even if the Type I mechanism remains the primary mechanism in two and three dimension, there still remains many questions in the full process. For example, the apparent density increase in test three has not been observed in the one dimensional test. While it seems likely that this is due to the convective burn organizing into the compact and compressing the material further down stream, the question remains if this effect will be seen in three dimensions. It is unclear if detonation breaks out at a point or simultaneously along a surface and this could have important implications for weapons response. Also, the effect of cracking of the explosive, especially consolidated PBX charges must be considered. It is unknown at this point if cracking will make DDT more or less likely. More testing needs to be pursued to address these possibilities. These effects and more must be understood before any real attempt at modeling a full three dimensional DDT response is attempted.

## References

- [1] P. W. Cooper. *Explosive Engineering*. Wiley-VCH, 1996.
- [2] T. Feagin, E. M. Heatwole, and P. Rae. "Investigating the minimum post-burst energy required to function an exploding bridgewire detonator. *Journal of Applied Physics*, submitted.
- [3] T. Feagin, E. M. Heatwole, and P. Rae. Time-resolved nanosecond optical pyrometry of the vapor-to-plasma transitions in exploding bridge-wires. *Scientific Review*, submitted.
- [4] A. Obmenin, A. Korotkov, A. Sulimov, and V. Dubovitskii. Propagation of predetonation regimes in porous explosives. *Fizika Gorenija i Vzryva*, 5:461–470, 1969.
- [5] G. R. Parker, E. M. Heatwole, M. D. Holmes, B. W. Asay, P. M. Dickson, and J. M. McAfee. Deflagration-to-detonation transition in hot hmx and hmx-based polymer-bonded explosives. *Combustion and Flame*, 215:295–308, 2020.